Detection of volcanic, solar and greenhouse gas signals in paleo-reconstructions of Northern Hemispheric temperature

Gabriele C. Hegerl,[1] Thomas J. Crowley,[1] Steven K. Baum,[2] Kwang-Yul Kim,[3] and William T. Hyde[1]

Received 19 November 2002; revised 10 January 2003; accepted 3 February 2003; published 12 March 2003.

[1] We apply a multiple regression method to estimate the response to anthropogenic and natural climate forcings simultaneously from a number of paleo-reconstructions of Northern Hemispheric average temperature. These long records (600 to 1000 years) provide a unique opportunity to distinguish between different external influences on climate. The response to volcanic forcing is reliably detected in all reconstructions, and the simulated temperature response to volcanic eruptions compares favorably with observations. The response to solar forcing is detected in Hemispheric mean data only over some periods in some records, and appears weak. Although most records can be used only to the middle of the 20th century, the temperature response to CO_2 can be detected by this time in most records. *INDEX TERMS:* 1699 Global Change: General or miscellaneous; 3344 Meteorology and Atmospheric Dynamics: Paleoclimatology; 1650 Global Change: Solar variability; 1620 Global Change: Climate dynamics (3309). **Citation:** Hegerl, G. C., T. J. Crowley, S. K. Baum, K.-Y. Kim, and W. T. Hyde, Detection of volcanic, solar and greenhouse gas signals in paleo-reconstructions of Northern Hemispheric temperature, *Geophys. Res. Lett.*, *30*(5), 1242, doi:10.1029/2002GL016635, 2003.

1. Introduction

[2] Results from recent detection and attribution studies based on 20th century instrumental data yield an increasing confidence in the detection of the anthropogenic greenhouse gas signal in 20th century temperature records [see, *Mitchell et al.*, 2001]. One of the key uncertainties of detection efforts based on instrumental data is that estimates of internal climate variability need to be derived from simulations with coupled climate models, and that the interdecadal to secular variability of climate models cannot be easily validated. Paleoclimatic data over several centuries provide a framework to consider both forced climate change and observed internal climate variability. The length of the records also enables better separation of the influence of different external forcings on climate, thus providing better estimates of the temperature response, particularly to natural climate forcing, such as volcanism and changes in solar radiation [cf. *Tett et al.*, 1998].

[3] Studies based on paleoclimatic data indicate a role of solar and volcanic forcing [e.g., *Mann et al.*, 1998; *Free and Robock*, 1999; *Crowley*, 2000; *Shindell et al.*, 2001]. Fingerprint detection methods (see below) are particularly suitable to reliably distinguish the influence of all relevant external influences from each other and from climate variability [see *Mitchell et al.*, 2001]. Here, we apply such a method to the detection and attribution of natural and anthropogenic forcings in a range of reconstructions of temperature over the past 6 to 10 centuries.

2. Detection Method

[4] We apply a multiple regression approach to detect and estimate fingerprints of anthropogenic forcing in paleo-reconstructions of Northern Hemispheric mean temperature. Such methods have been successfully applied to the detection of 20th century temperature change and its attribution to anthropogenic and natural forcings [e.g., *Hegerl et al.*, 1997; *Tett et al.*, 1998]. The observed record is linearly composed from a number of externally forced signals (here, the climate response to volcanism, solar forcing, and a combination of greenhouse gases and sulfate aerosols), and the residual is attributed to internal climate variability. The shape of the externally forced signal (''fingerprint'', here its time evolution) is derived from simulations with a climate model (here an energy balance model, ''EBM''). The amplitude of the signal is estimated from observations. If the amplitude of a signal is significantly different from zero, then the signal is ''detected''. If a signal amplitude of ''1'' is within the uncertainty range, the model signal is consistent with observations. Only if all signals with a substantial presence in the observed record are considered simultaneously can the observed climate variations be reliably attributed to external forcings and climate variability.

[5] The uncertainty range for the amplitude estimate is based on variations in fingerprint amplitudes that arise from internal climate variability and random errors in the reconstructions (''noise''). Noise samples are based on the residual proxy-timeseries after subtracting the best estimate of the externally forced signals. To provide a large sample, the residual timeseries has been shifted by increments of one year (appending the cut-off from the beginning at the end), yielding as many samples as years in the record, each of them of the same length as the record. The effective sample size is limited due to autocorrelation, its estimate (after subtracting three for fitting three time series to the data) typically exceeds 20 samples for entire records. The residual timeseries generally agree with a Gaussian distribution, and the resulting confidence limits are nearly identical if Monte-Carlo simulations of a fitted red-noise process are used. In a

[1]Nicholas School of the Environment and Earth Sciences, Duke University, Durham, North Carolina, USA.
[2]Department of Oceanography, Texas A&M University, College Station, Texas, USA.
[3]Department of Meteorology, Florida State University, Talahassee, Florida, USA.

0094-8276/03/2002GL016635$05.00

few cases, the residual exhibits unusually large trends over some period that cannot be explained by the forcings. Results then need to be treated with caution.

[6] The results of the detection analysis are sensitive to the accuracy of the simulated climate response to forcing, and errors in the forcing and paleo reconstruction. Errors in the *amplitude* of forcing, EBM response or paleo reconstruction do not influence the detection of signals, but will bias the scaling required to best fit observations. Errors in the *shape* of the fingerprint and proxy-timeseries will, however, lead to low estimates of the signals and possibly prevent their detection.

3. Observations

[7] We utilized a range of proxy-based reconstructions for Northern Hemispheric temperature evolution. Among them are records based on tree ring data only [*Briffa et al.*, 2001, hereinafter referred to as B01; *Esper et al.*, 2002, hereinafter referred to as E02]. Both records are based on tree ring data which have been standardized using an average age curve (such as "Age banding" in B01 and "Regional Curve Standardization" in E02). This preserves decadal and secular variability better than the earlier used individual age model [cf. *Briffa et al.*, 1998]. B01 is a record of Northern Hemisphere (NH) 20N–90N growing season (April–September) land temperature; the dimensionless record E02 has been also scaled to the NH growing season average over land.

[8] We also consider the *Mann et al.* [1999, hereafter referred to as M99] multi-proxy reconstruction of annual NH temperature (0–90N) and a modified version [*T. J. Crowley et al.*, in preparation, "CLH"] of the *Crowley and Lowery* [2000, hereinafter referred to as CL00] reconstruction (correlation with CLH 0.94). The latter is a weighted average of 9 long decadal or decadally averaged records over the Northern Hemisphere mid-to-high latitudes (30–90 N, the records sample both the warm and cold season, with a likely bias towards the summer half year). The weights are determined from the regression coefficients of individual records with the 30–90 N annual mean instrumental record during the period of overlap [*Jones et al.*, 1999]. The resulting paleo time series was scaled so that the regression fit with the instrumental data from 1880–1960 had a slope of 1.0 [decadal correlations of 0.81 (with trend) and 0.66 (detrended)]. For consistency, the scaling of E02 is based on the same period and also decadally filtered data.

[9] There is good qualitative agreement between the reconstructions - all show a more or less pronounced Medieval warm period, warm intervals for most of the 16th and 18th century, a cool 17th and early 19th century, and a temperature rise in the early 20th century. However, the amplitude and timing of fluctuations varies between records [cf. *Briffa and Osborn*, 2002].

4. Model and Forcing Time Series

[10] Ideally, fingerprints for external climate forcing are derived from large ensembles of general circulation model (GCM) simulations driven by variations in individual forcings over 600–1000 years. However, such simulations are not yet available. EBM simulations reproduce many aspects of the large-scale temperature response of GCMs

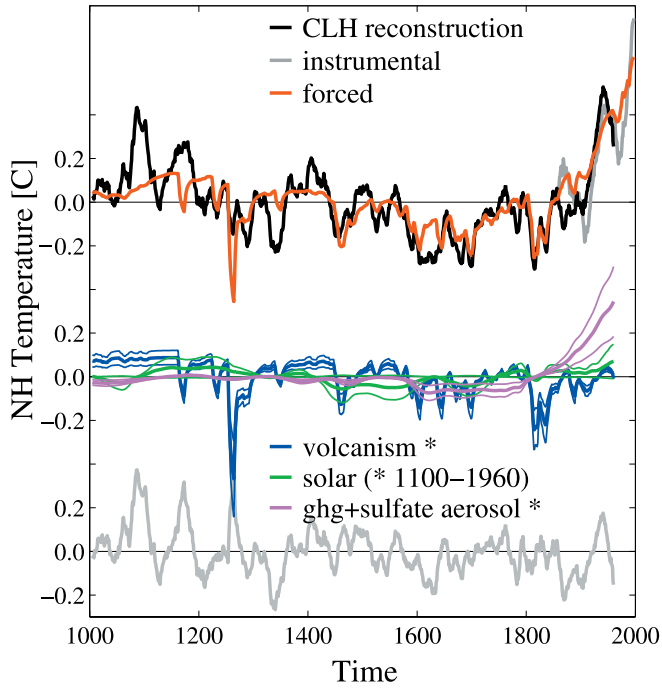

Figure 1. Detection results for the updated *Crowley and Lowery* [2000] reconstruction of decadal Northern Hemispheric mean temperature (north of 30N, calendar year average). Upper panel: Paleo reconstruction (black) compared to the instrumental data (grey) and the best estimate of the combined forced response (red), middle panel: response attributed to individual forcings (thick lines) and their 5–95% uncertainty range (thin lines), lower panel: residual variability attributed to internal climate variability and errors in reconstruction and forced response. An asterisk "*" denotes a response that is detected at the 5% significance level.

to radiative forcing without influence from internal climate variability. Previously, hemispheric mean temperature reconstructions [e.g., M99, CL00] were compared with EBM simulations for the whole Northern Hemisphere [*Free and Robock*, 1999; *Crowley*, 2000]. Since most paleoclimatic data are from the mid- and high-latitudes of the Northern Hemisphere, we employ here a linear North-type [*North et al.*, 1983] 2D (i.e., realistic land-sea distribution) seasonal model to compare the model results over the same season and the same subsection of the Northern Hemisphere that is covered by the data (for example, land only records based on data from 20–90 N are compared with EBM land data from the same latitude strip). The EBM responds similarly as GCMs to changes in boundary conditions, including the seasonal cycle of insolation [*Crowley et al.*, 1991] and shows a similar response to volcanism in the late 20th century [cf. *Stott et al.*, 2000].

[11] The sensitivity of the EBM is set to 2.5 K for CO2 doubling in the present study, since a sensitivity between 2 and 3 yielded reasonable agreement between the amplitude of combined forcing simulations and the CLH paleodata [T. J. Crowley et al., in preparation]. The model is driven by external forcing changes in greenhouse gases, solar irradiance, volcanism, and tropospheric aerosols. The greenhouse gas and solar forcing used in the present study are from

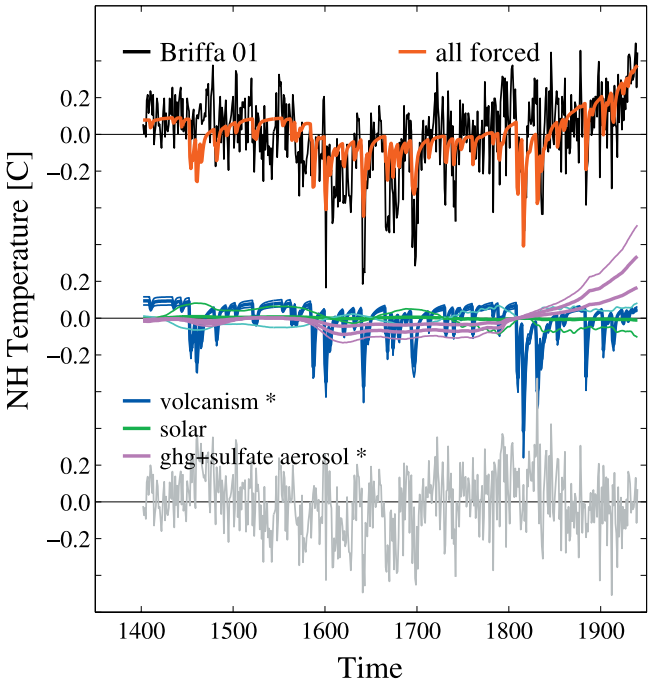

Figure 2. As Figure 1, but based on the *Briffa et al.* [2001] reconstruction of NH growing season temperature (April through September) over land (north of 20 N) 1402 to 1940.

Crowley [2000]. We employ an aerosol forcing of 0.5 W/m^2 for 30–90 N from 1900 on, and 0.3 W/m^2 from 0–30 N. The sulfate aerosol fingerprint is added to the greenhouse gas only fingerprint and then both are estimated together. Results proved insensitive to doubling or omitting the aerosol fingerprint except for a small variation in the estimate of the combined signal.

[12] The volcano forcing time series used in *Crowley* [2000] has been slightly revised [*T. J. Crowley et al.*, in preparation]. In addition to ice core data used previously, we factored in the assessment of *Robock and Free* [1996]. The ice core Aerosol Optical Depth (AOD) was initially determined by matching the 1883 Krakatau peak in the ice cores to the instrumental AOD record [*Sato et al.*, 1993]. Because there is considerable uncertainty about the absolute value of Krakatau AOD estimates, the preliminary scaling for 1900–1960 was validated against the presumably more-reliable 30–90 N 1900–1960 portion of the AOD record. The aerosol optical depth was converted to radiative forcing using a factor of 30 [*Sato et al.*, 1993] determined by detailed radiative convective modeling. A volcano catalog [*Simkin and Siebert*, 1994] was used to assign tentative sources to many of the eruptions. Unknown ice core peaks in the pre-anthropogenic record were assigned a high latitude (>50°) origin unless they could be verified in ice cores from Antarctica [see *Crowley*, 2000]; thus minimizing the effects of ice core volcano peaks unless their larger-scale imprint can be verified from independent data. This proxy-reconstruction agrees in general with other reconstructions of volcanic forcing, and has an estimated uncertainty of ca. 50%.

5. Results

[13] Figure 1 shows the estimated contribution of solar, volcanic and greenhouse gas forcing to the CLH record, and Figure 2 to the B01 record. A comparison of signal estimates and detection results between the different reconstructions is given in Table 1. Results using different reconstructions compare favorably. The results are dominated by low frequency aspects of the signals (low-pass filtering the annual/seasonal data yielded nearly identical results). In all cases, the volcanic signal is highly significant. A CO_2/aerosol signal is detected in B01 (although this record can only reliably be used to 1940), in CLH and E02 by 1960 (Table 1), and in M99 by 1980 (not shown).

[14] Attributed signal amplitudes are generally consistent between analysis periods (c.f. Table 1). The observed response to volcanic forcing is consistent with the model simulations in B01, CLH and E02 and tends to be smaller than simulated in M99. This may be, at least partly, due to dynamically induced winter warming [*Robock and Mao*, 1992] which reduces the effect of volcanism on annual means. The greenhouse gas signal is larger than simulated in E02 and smaller than simulated in M99. The residual from the M99 record, after analyzing a period encompassing the 19th century, shows a large fluctuation not explained by either forcing. A possible reason is that the response to other external influences, such as land use change, has a stronger influence on M99 than the other records and disturbs the agreement between simulations and observations. If this period is omitted from the analysis, the estimates of the contributing forcings are generally larger.

[15] Solar signals with an amplitude that is consistent with simulations are detected in a two-way regression between solar and volcanic signals between 1000 and 1830 in M99 and in CLH. However, if the CO_2 forcing is included in the analysis, some of the Maunder mimimum cooling gets attributed to a small drop in CO_2 (c.f. Figures 1–2. In that case, the response to solar forcing is only

Table 1. Estimated signal amplitudes (unit-less) as scaling factors by which energy balance model simulations need to be scaled for best agreement with observations ("1" indicates a correct amplitude of the simulation) and 5–95% uncertainty levels. Signals that are detected at the 5% significance level (one-sided) are shown in bold, an arrow "↓" ("↑") denotes that the signal amplitude is significantly smaller (larger) than simulated. B01 refers to the *Briffa et al.* [2001] record, CLH to the updated *Crowley and Lowery* [2000] record, M99 to the *Mann et al.* [1999] data and E02 to the *Esper et al.* [2002] record, the period of the analysis is given in the second row. The bottom row lists the standard deviation (K) of the (decadally smoothed for annual records) residual, and the percent variance explained by the external forcing (in parentheses).

Record	B01	CLH	M99	E02	CLH
Period	1400–1940	400–1960	1400–1960	1400–1960	1000–1960
volcano	**0.92 ± 0.21**	**1.22 ± 0.39**	**0.63 ± 0.23** ↓	**1.01 ± 0.34**	**1.14 ± 0.40**
solar	−0.1 ± 0.83 ↓	0.18 ± 0.48 ↓	0.43 ± 0.61	−0.18 ± 0.96↓	0.63 ± 0.67
ghg + aer	**1.11 ± 0.55**	**1.13 ± 0.26**	0.26 ± 0.35 ↓	**1.88 ± 0.57** ↑	**0.96 ± 0.42**
res std.	0.09 (57%)	0.08 (77%)	0.07 (49%)	0.13 (67%)	0.10 (57%)

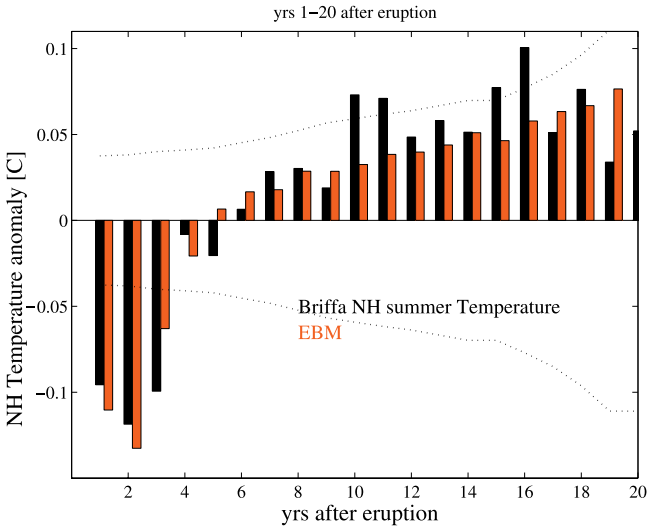

Figure 3. Comparison of the average response to volcanic eruptions in the energy balance model and the *Briffa et al.* [2001] reconstruction from the year of the eruption (year 1) to the next major eruption. 5–95% uncertainty ranges for the observed response are given by the dotted lines (note that sample size decreases with time).

detectable in segments of M99 and in CLH 1100–1960. It is possible that annual averaging and the wintertime dynamical response [*Shindell et al.*, 2001] helps in the detection of the solar signal, particularly in M99.

[16] The EBM response tends to associate inter-decadal temperature variations with periods of unusually heavy or weak volcanism. A similar tendency occurs in coupled climate models, [e.g., *Stott et al.*, 2000]. In order to assess if such a simulated response is realistic, we have conducted a superposed epoch analysis by averaging the temperature response after 50 major volcanic eruptions between 1400 and 1940 (Figure 3). The average considers only the response before the next major eruption. To avoid contamination by other external forcing, the estimated solar and greenhouse gas signal has been subtracted from the observations prior to the analysis (result not sensitive to taking solar forcing into account). The observations show a significant cooling in the first three years of the eruption, which compares very favorably to the magnitude and duration of the simulated response. Afterwards, a marginally significant temperature increase reflects the relaxation to an equilibrium climate state without volcanic forcing in model and data. The results of this analysis are qualitatively confirmed if the *Briffa et al.* [1998] data or the M99 record is used.

6. Conclusions

[17] The response to volcanic forcing is reliably detected in all reconstructions of Northern Hemispheric mean temperature considered, and the simulated timescale of temperature response to volcanic eruptions compares very favorably with observations. Although most records can be only used to the middle of the 20th century, the temperature response to CO_2 can be detected by then in most records (in all by 1980). The response to solar forcing is detected only over some periods in some records. The overall impression is that solar variability plays a relatively modest role in multi-decadal climate variability of hemispherically averaged temperature. The early 20th century warming is attributed to a composite of greenhouse warming, an uncertain contribution from solar forcing, and a recovery from a previous period of heavy volcanism.

[18] **Acknowledgments.** This work has been supported by NOAA grant NA16GP2242 and by NOAA's office of global programs and the DOE's Office of Biological and Environmental Research. GCH is also supported by the Nicholas School of the Environment and Earth Sciences and by NSF grant 0296007. We thank Phil Jones, Keith Briffa, Mike Mann and Ed Cook for valuable discussions and assistance, and two anonymous reviewers for their valuable comments.

References

Briffa, K. R., and T. Osborn, Blowing hot and cold, *Science*, *295*, 2227–2228, 2002.
Briffa, K. R., P. D. Jones, F. H. Schweingruber, and T. J. Osborn, Influence of volcanic eruptions on Northern Hemisphere summer temperature over the past 600 years, *Nature*, *393*, 450–454, 1998.
Briffa, K. R., et al., Low-frequency temperature variations from a northern tree ring density network, *J. Geophys. Res.*, *106*, 2929–2941, 2001.
Crowley, T. J., Causes of climate change over the last 1000 years, *Science*, *289*, 270–277, 2000.
Crowley, T. J., and T. S. Lowery, How warm was the medieval warm period, *Ambio*, *29*, 51–54, 2000.
Crowley, T. J., S. K. Baum, and W. T. Hyde, Climate model comparison of Gondwanan and Laurentide glaciations, *J. Geophys. Res.*, *96*, 9217–9226, 1991.
Esper, J., E. R. Cook, and F. Schweingruber, Low-frequency signals in long tree-ring chronologies for reconstructing past temperature variability, *Science*, *295*, 2250–2253, 2002.
Free, M., and A. Robock, Global warming in the context of the little Ice Age, *J. Geophys. Res.*, *104*, 19,057–19,070, 1999.
Hegerl, G. C., Multi-fingerprint detection and attribution analysis of greenhouse gas, greenhouse gas-plus-aerosol and solar forced climate change, *Clim. Dyn.*, *13*, 613–634, 1997.
Jones, P. D., M. New, D. E. Parker, S. Martin, and I. G. Rigor, Surface air temperature and its changes over the past 150 years, *Rev. Geophys.*, *37*, 173–199, 1999.
Mann, M. E., R. S. Bradley, and M. K. Hughes, Global-scale temperature patterns and climate forcing over the past six centuries, *Nature*, *392*, 779–787, 1998.
Mann, M. E., R. S. Bradley, and M. K. Hughes, Northern Hemisphere temperatures during the past millenium: Inferences, uncertainties and limitations, *Geophys. Res. Lett.*, *26*, 759–762, 1999.
Mitchell, J. F. B., et al., Detection of climate change and attribution of causes, in *Climate Change 2001: The Scientific Basis*, edited by J. T. Houghton et al., 881p., Cambridge Univ. Press, New York, 2001.
North, G. R., J. G. Mengel, and D. A. Short, Simple energy balance model resolving the seasons and the continents: Application to the astronomical theory of Ice Ages, *J. Geophys. Res.*, *88*, 6576–6586, 1983.
Robock, A., and M. P. Free, The volcanic records in ice cores for the past 2000 years, in *Climatic Variations and Forcing Mechanisms of the Past 2000 years*, edited by P. D. Jones, R. S. Bradley, and J. Jouzel, pp. 533–546, Springer-Verlag, New York, 1996.
Robock, A., and J. Mao, Winter warming from large volcanic eruptions, *Geophys. Res. Lett.*, *19*, 2405–2408, 1992.
Sato, M., J. E. Hansen, M. P. McCormick, and J. B. Pollack, Stratospheric aerosol optical depths (1850–1990), *J. Geophys. Res.*, *98*, 22,987–22,994, 1993.
Shindell, D. T., G. A. Schmidt, M. E. Mann, D. Rind, and A. Waple, Solar forcing of regional climate change during the Maunder Minimum, *Science*, *294*, 2149–2152, 2001.
Simkin, T., and L. Siebert, *Volcanoes of the World*, 2nd ed., Geosciences, Tucson, Ariz., 1994.
Stott, P. A., et al., External control of twentieth century temperature variations by natural and anthropogenic forcings, *Science*, *15*, 2133–2137, 2000.
Tett, S. F. B., P. A. Stott, M. R. Allen, W. J. Ingram, and J. F. B. Mitchell, Causes of twentieth century temperature change, *Nature*, *399*, 569–572, 1998.

S. K. Baum, Department of Oceanography, Texas A&M University, College Station, TX, USA.
T. J. Crowley, G. C. Hegerl, and W. T. Hyde, Department of Earth and Ocean Sciences, Nicholas School of the Environment and Earth Sciences, Duke University, Durham, NC 27708, USA. (hegerl@duke.edu)
K.-Y. Kim, Department of Meteorology, Florida State University, Talahassee, FL, USA.